Optimal Thrust Control of a Missile with a Pulse Motor

Fumiaki Imado* and Takeshi Kuroda†
Mitsubishi Electric Corporation, Hyogo, 661 Japan
and
Susumu Miwa‡
Tokyo Denki University, Tokyo, 101 Japan

Optimal thrust control of a missile with a realistic pulse motor for midcourse guidance is proposed. First, the optimal thrust pattern that maximizes the missile's final velocity is calculated by solving a nonlinear two-point boundary value problem. Second, the way of implementing this pattern with a realistic pulse motor is studied. The result shows that the optimal thrust pattern is well approximated by a two-pulse type rocket motor. The optimization of the two-pulse control and the comparison with single-thrust control are studied and discussed.

Nomenclature

C_D, C_L = drag and lift coefficients, respectively
C_{D0} = zero-lift drag coefficient
$C_{L\alpha}$ = $\partial C_L/\partial\alpha$
D = drag
g = acceleration of gravity
h = altitude
I_{sp} = specific impulse
k = induced drag coefficient
L = lift
M = Mach number
m = mass
s = reference area
T = thrust
t, t_f = time and terminal time, respectively
v = velocity
x = down range
α, α_0 = angle of attack and zero-lift angle
γ = flight-path angle
ρ = air density
ϕ = performance index function
Ω = stopping condition

Subscripts

f = terminal value
max = maximum value

Superscript

$(\cdot)$ = time derivative

Introduction

MANY studies have been performed on the optimal thrust control of aircraft, but only a few have been conducted on tactical missiles. The reason is thought to be the lack of freedom on the thrust control of such missiles, since they usually employ solid rockets. A typical tactical missile employs a combination of a booster and a sustainer to acquire an initial speed and to maintain its velocity, respectively. Considering the current technique of making solid rocket motors, the freedom of designing an arbitary thrust pattern has been very limited.

Recently, the use of a pulse motor has somewhat changed the situation. That is, the pulse motor can control the ignition interval between two pulses, which can give some freedom on missile velocity control. Hardtla et al. studied the optimal ignition time of a pulse motor by employing the linear quadratic regulator (LQR).[1] Calise and Jonnalagada obtained minimum-time flight trajectories of a pulse rocket by employing the maximum principle.[2] Menon et al. obtained maximum range flight trajectories by employing the quasi-Newtonian parameter optimization method.[3] These studies showed the possibility of improving the missile performance by optimizing the pulse motor control.

Our preceding study showed the importance of the final velocity of midcourse guidance to intercept a highly maneuverable target.[4] Thus we were motivated to maximize the missile final velocity by using a pulse motor. We have solved the optimal pulse motor control problem of a medium-range tactical missile by employing the steepest ascent method. Particular emphasis was laid on the applicability of the obtained control law to an actual missile.

In this paper, the mathematical model of a conceptual medium-range surface-to-air missile is shown first. Second, the angle of attack α and the thrust T of the missile are simultaneously optimized with several prespecified final positions. Third, the optimal pattern of the thrust was replaced by a two-pulse-type rocket motor, and its characteristics and performance are discussed. Finally, the optimal fuel distribution and the ignition interval of the pulses are analyzed, and the effectiveness is compared with that of a single-stage motor.

Mathematical Model

The missile is modeled as a point mass in the study. The superiority of a point-mass model to reduced-order models is well described by Katzir et al.[5] The data are almost the same as those of Ref. 4, although total fuel weight is slightly increased to accommodate a surface-to-air missile.

Figure 1 shows missile force balance as well as the symbols employed in this paper. For simplicity, motions are constrained within a vertical plane. The missile is modeled as a point mass, and the equations of motion are

$$\dot{v} = (T\cos\alpha - D)/m - g\sin\gamma \tag{1}$$

$$\dot{\gamma} = (L + T\sin\alpha)/(mv) - (g/v)\cos\gamma \tag{2}$$

Received July 7, 1989; presented as Paper 89-3479 at the AIAA Guidance, Navigation, and Control Conference, Boston, MA, Aug. 14–16, 1989; revision received Feb. 14, 1990.

*Chief Engineer, Advanced Mechanical Systems Department, Central Research Laboratory, Amagasaki Hyogo. Member AIAA.
†Engineer, Advanced Mechanical Systems Department, Central Research Laboratory, Amagasaki Hyogo.
‡Professor, Department of Electrical Communication Engineering, Faculty of Engineering, Kanda Chiyoda-ku Tokyo.

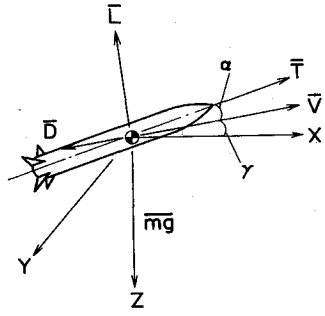

Fig. 1 Missile force balance and symbols.

$$\dot{x} = v\cos\gamma \tag{3}$$

$$\dot{h} = v\sin\gamma \tag{4}$$

$$\dot{m} = -T/(g\,I_{sp}) \tag{5}$$

where

$$L = 1/2\,\rho v^2 s\,C_L, \qquad C_L = C_{L\alpha}\,(\alpha-\alpha_0) \tag{6}$$

$$D = 1/2\,\rho v^2 s\,C_D, \qquad C_D = C_{D0} + k\,C_L{}^2 \tag{7}$$

The aerodynamic derivative coefficients $C_{L\alpha}$, C_{D0} and k are given as functions of Mach number M, which is a function of v and h, and the air density ρ is a function of h:

$$\rho = \rho(h), \qquad M = M(v, h) \tag{8}$$

$$C_{L\alpha} = C_{L\alpha}(M), \qquad C_{D0} = C_{D0}(M), \qquad k = k(M) \tag{9}$$

Some parameters employed in the study are shown in Table 1. The drag coefficients in boosting are generally smaller than those of coasting, but the differences are neglected here.

The optimal midcourse trajectory is obtained by maximizing the following performance index ϕ, in relation to the missile angle of attack $\alpha(t)$ and the thrust $T(t)$, under the equations of motion Eqs. (1-5),

$$\phi = v_{t_f} \tag{10}$$

with terminal constraints

$$\begin{bmatrix} x \\ h \end{bmatrix}_{t_f} = \begin{bmatrix} x_f \\ h_f \end{bmatrix} \tag{11}$$

where the terminal time t_f is determined from the stopping condition

$$\Omega \equiv m - m_f = 0 \tag{12}$$

The following constraints are imposed on the control variables:

$$-\alpha_{max} \le \alpha \le \alpha_{max} \tag{13}$$

$$0 \le T \le T_{max} \tag{14}$$

This problem can be solved by using the steepest ascent method.[6] Since the method is well known to the researchers of the field, only a short comment is stated about our computer program. To improve the convergence, the norm is increased or decreased automatically in a geometric ratio, depending on the success or failure of the iteration. An example of the convergence speed is shown in Fig. 2 where the ordinate is the performance index and the abscissa is the number of iteration.

Table 1 Missile parameters

Initial mass	m_0	= 240 kg
Final mass	m_f	= 132 kg
Reference area	S	= 0.03 m^2
Control limits	α_{max}	= 0.349 rad
	T_{max}	= 26400 N
Specific impulse	I_{sp}	= 200 or 250 s
Aerodynamic	$C_{L\alpha}$	= 35.0
parameters	C_{D0}	= 0.92
(at M = 2)	K	= 0.03
	α_0	= 0

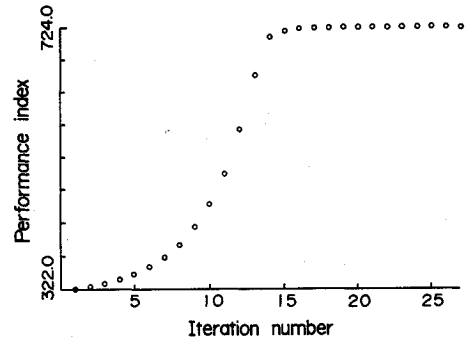

Fig. 2 An example of the convergence of iteration (performance index vs iteration numbers).

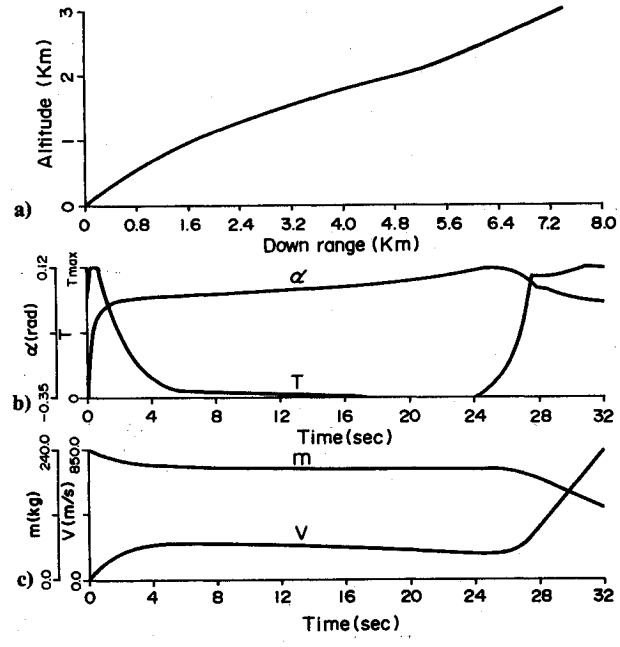

Fig. 3 Flight trajectory, control histories, and mass and velocity histories by optimal control (I_{sp} = 200 s, slant range 8 km).

Optimal Thrust Pattern

The optimal thrust patterns preceding from the preceding model are shown and discussed in this section. The initial and final masses of the missile are 240 and 132 kg, respectively. The missile is launched vertically, and its terminal altitude is set to 3 km; slant ranges are 8, 12, 18, and 30 km. The maximum value of T is limited to 26,400 N. The specific impulse I_{sp} of the missile is usually a function of thrust value, but the constant values of 200 and 250 s are employed in this paper.

Figures 3-7 show trajectories, control histories, and mass and velocity histories of the optimal trajectories for various slant ranges. The I_{sp} is set to 200 s in all these cases.

Figure 3 shows the case of the slant range of 8 km. Some portion of the total fuel is consumed at launch. Then the rest is consumed in the proximity of the terminal point. A higher missile velocity produces a larger aerodynamic drag, whereas the lower speed exposes a missile to the drag for a longer time. Therefore, an appropriate velocity for a missile will exist. In Fig. 3c, the velocity line is almost flat from 3 s through 26 s, which agrees with the conjecture. These patterns of thrust and velocity are common in optimal trajectories throughout this section. As no thrust vector control is employed in this study, the angle of attack α initially takes a large negative value to turn the missile trajectory, then takes a positive value to maintain a lift.

The missile gradually ascends to its terminal point as seen in Fig. 3a. This pattern is almost the same as the case of Fig. 4, where the slant range is set to 12 km. We have found that there are at least two types of local extremals in these kind of trajectories. One is the type shown in Figs. 3 and 4; the other is the type in which the missile initially takes a very high altitude and then gradually descends to a terminal point.[4]

Figure 5 shows that type of optimal trajectory that corresponds to the latter at the slant range of 12 km. The final velocities in the cases of Fig. 4 and Fig. 5 are 660 and 780 m/s, respectively. Therefore the latter is globally optimum. The type of global optimality depends on the slant range; the boundary is about 10 km in this situation.

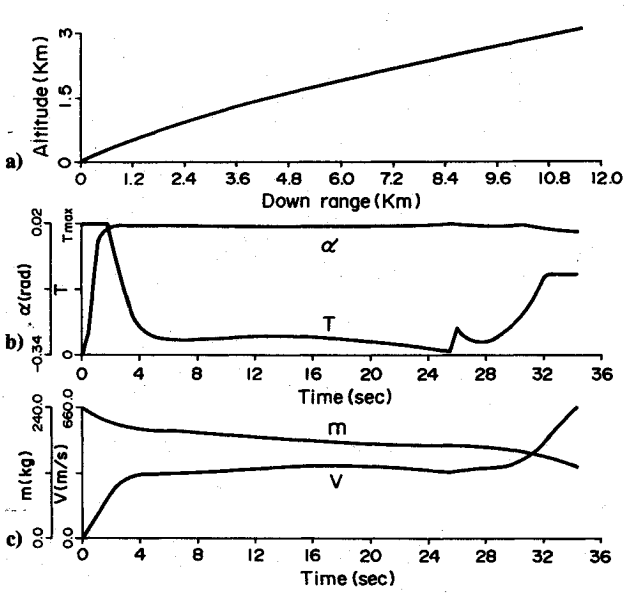

Fig. 4 Flight trajectory, control histories, and mass and velocity histories by optimal control I (I_{sp} = 200 s, slant range 12 km).

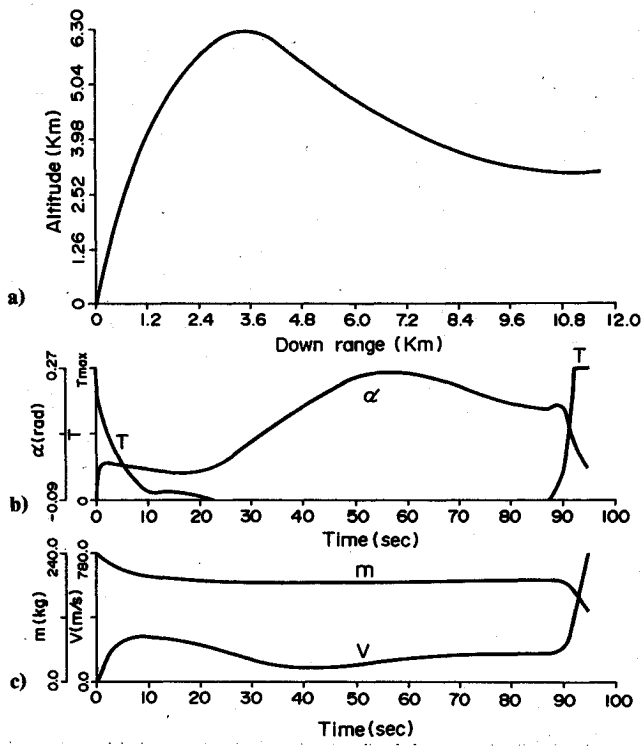

Fig. 5 Flight trajectory, control histories, and mass and velocity histories by optimal control II (I_{sp} = 200 s, slant range 12 km).

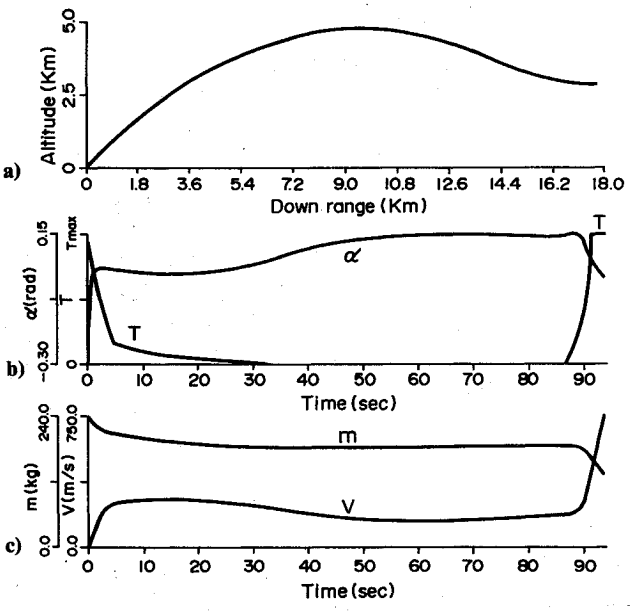

Fig. 6 Flight trajectory, control histories, and mass and velocity histories by optimal control (I_{sp} = 200 s, slant range 18 km).

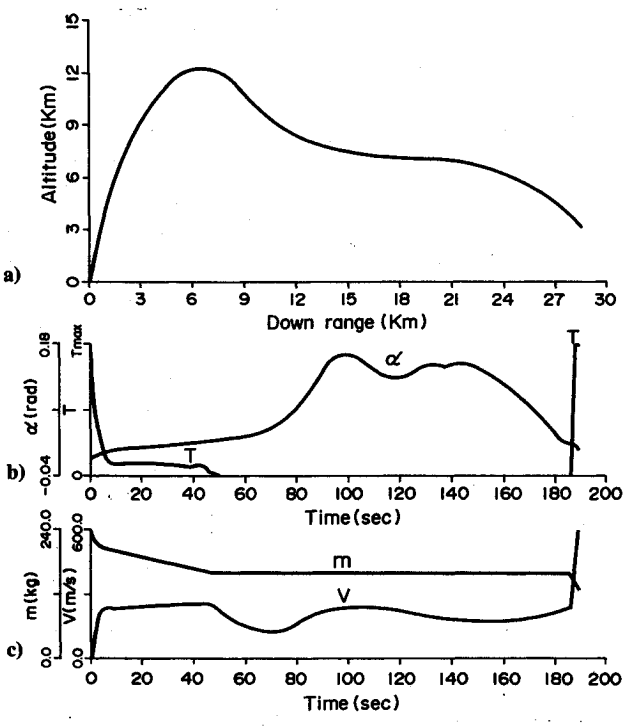

Fig. 7 Flight trajectory, control histories, and mass and velocity histories by optimal control (I_{sp} = 200 s, slant range 30 km).

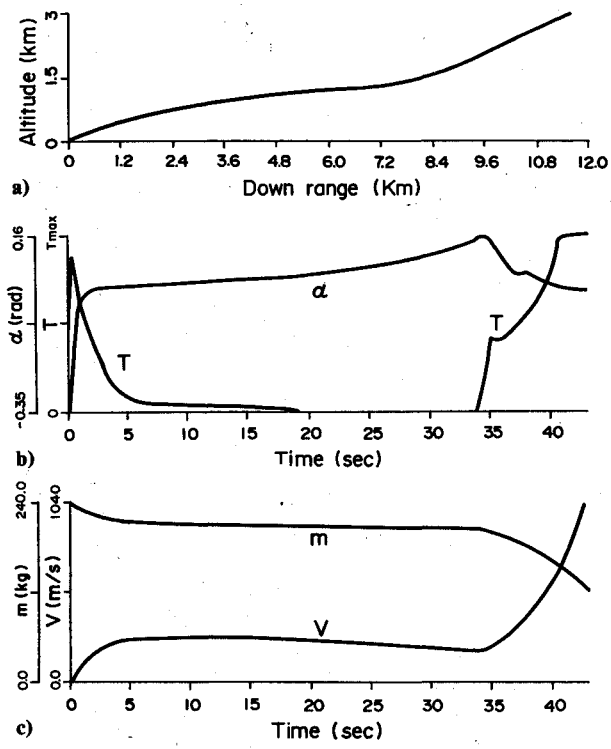

Fig. 8 Flight trajectory, control histories, and mass and velocity histories by optimal control (I_{sp} = 250 s, slant range 12 km).

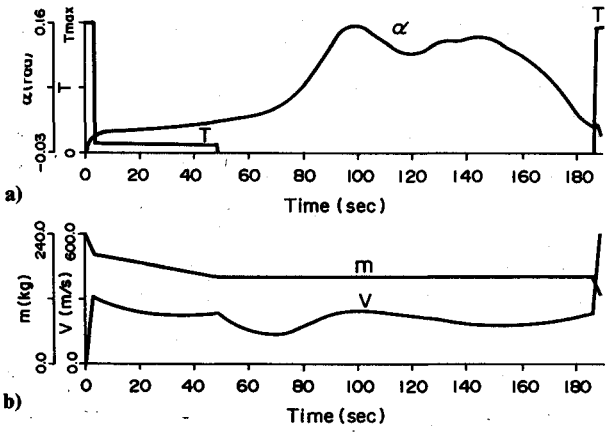

Fig. 9 Control histories and mass and velocity histories by a pulse motor (booster + sustainer + booster, I_{sp} = 200 s, slant range 30 km).

Figures 6 and 7 show the cases of the slant range of 18 and 30 km, respectively. The angle of attack α is almost constant in Fig. 6, whereas α is small in the first part and becomes large in the latter half in Fig. 7. The obtained final velocities corresponding to the slant range of 12, 18, and 30 km are 780, 750, and 600 m/s, respectively.

Similar studies were conducted for I_{sp} of 250 s. Naturally, the final velocities are largely increased compared with 200-s I_{sp} cases. Only one example is shown here in Fig. 8 for a slant range of 12 km. This corresponds to Fig. 4 for I_{sp} = 200 s. The final velocity of 1040 m/s is attained in Fig. 8, compared with 660 m/s in Fig. 4.

Implementation of Optimal Thrust Pattern by a Pulse Motor

Although the optimal thrust pattern obtained in the preceding section may be most effective, it is difficult to implement using a solid rocket motor with existing technology. Therefore, we tried to approximate these thrust patterns by a pulse motor. Some study results will be shown and discussed.

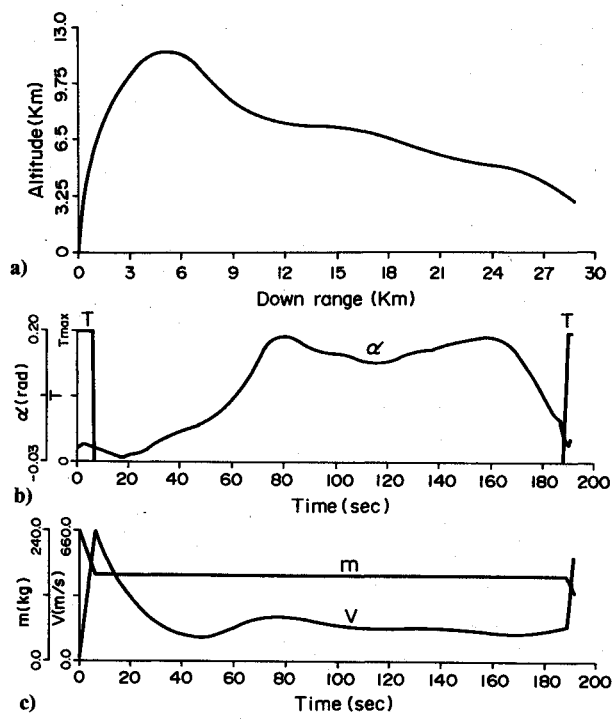

Fig. 10 Flight trajectory, control histories, and mass and velocity histories by a pulse motor (two pulses, I_{sp} = 200 s, slant range 30 km).

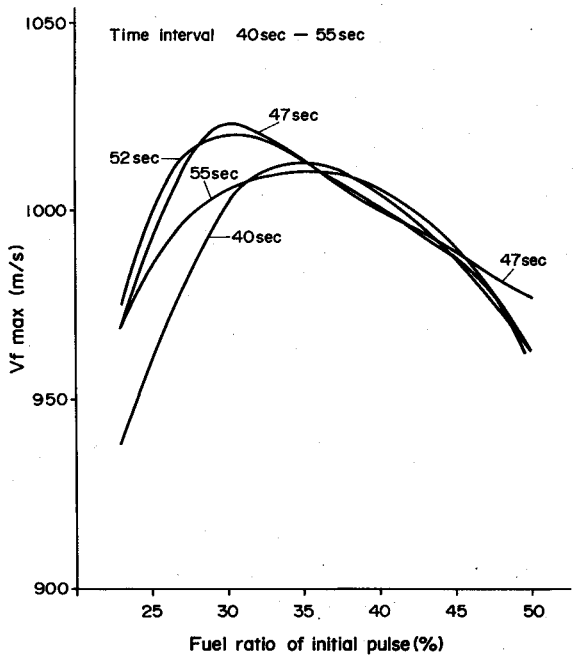

Fig. 11 Initial impulse ratio, ignition interval vs final velocity (two pulses, I_{sp} = 250 s, slant range 12 km).

The thrust patterns of Figs. 3-8 give us an insight that they will be approximated by a booster and sustainer and another booster. This is most clearly seen in Fig. 7. The thrust pattern of Fig. 7 is reshaped as shown in Fig. 9, considering the centroid of the impulse. The results using this thrust pattern are also shown in Fig. 9, where only the angle of attack α must be optimized. The final velocity of Fig. 9 is 600 m/s, almost the same value as that of Fig. 7. Therefore, if this type of a pulse motor would be realized, then the optimal thrust pattern will be well approximated.

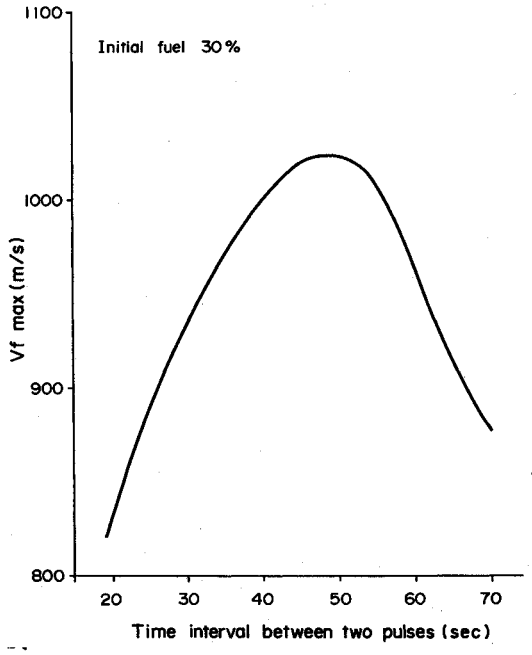

Fig. 12 Ignition interval vs final velocity by a pulse motor (two pulses, initial impulse ratio 30%, I_{sp} = 250 s, slant range 12 km).

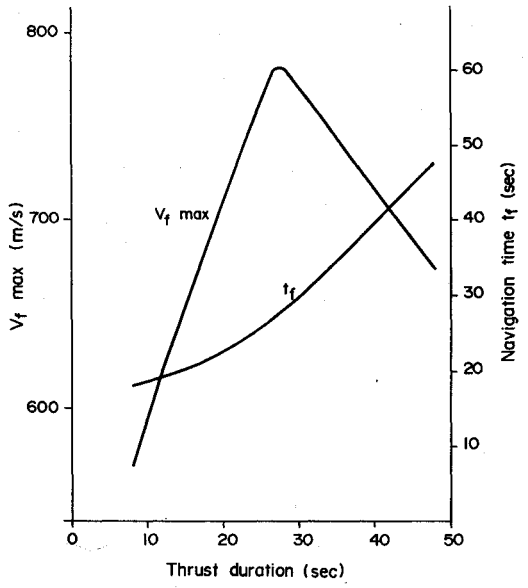

Fig. 13 Thrust duration vs final velocity and navigation time by a single-stage motor (I_{sp} = 250 s, slant range 12 km).

However, a more practical pulse motor will be the one that can only adjust the ignition interval between two pulses. Figure 10 shows the case where the thrust pattern is approximated by two pulses of the same magnitude. The impulse rate of the first and the second pulses and the interval time are optimized simultaneously with the α history. The obtained final velocity is 540 m/s in this case, which is 10% less than that of Fig. 7 or Fig. 9. We must admit that a two-pulse-type rocket motor provides only a suboptimal solution for controlling the missile final velocity in the midcourse region. However, this type of pulse motor seems to be most practical, and it will be useful to study parametric optimization on two-pulse control. We have studied the optimal impulse ratio and interval, which will be shown in the next section.

Optimal Two-Pulse Control by a Pulse Motor

The final velocity obtained with two-pulse control is largely changed with the impulse ratio of the two pulses and with the ignition interval between them. Let us take an example from Fig. 8 where the I_{sp} and slant range are set to 250 s and 12 km. The thrust pattern is approximated by two pulses, and the angle of attack α is optimized to maximize the missile final velocity.

Figure 11 shows the final velocity vs the impulse ratio of the initial pulse (first impulse divided by total impulse) for the ignition intervals of 40, 47, 52, and 55 s. The maximum final velocity is attained when the impulse ratio is 30% and the interval is around 50 s.

Figure 12 shows the final velocity in relation to the ignition interval for the case where the impulse ratio is a constant of 30%. More than 1000 m/s is attained at the interval between 39 and 56 s, which is 4% less than the maximum value of Fig. 8 and also only 2.4% less than the maximum value in Fig. 11. As a missile has to maintain a velocity until the ignition time of the second pulse, the optimal impulse ratio naturally increases as the slant range increases. But the impulse ratio cannot be changed for a pulse motor; therefore it must be designed for the maximum range of the missile. However, by adjusting the ignition interval and suitably controlling the angle of attack, a fairly large final velocity can be attained by a pulse motor.

To show the effectiveness of a pulse motor compared to a single-stage motor, another result is shown. Figure 13 shows the relation between the final velocity by a single-stage motor and the thrust duration, keeping the total impulse constant. The I_{sp} and slant range are same as that of Fig. 11. The navigation time t_f is also shown for a reference. The maximum value of v_f is 780 m/s, which is about 25% less than the maximum value of 1040 m/s attained by a pulse motor.

Conclusions

The optimal thrust pattern that maximizes the final velocity in the midcourse phase of a medium-range tactical missile and the way of implementing the pattern by a pulse motor have been studied and discussed.

In the optimal thrust analysis, it was found that there are two types of local optimum solutions. One is globally optimum at a slant range less than 10 km, where the missile gradually ascends to the terminal point. Another is globally optimum at a slant range larger than 10 km, where the missile first takes high altitude, then gradually descends to the terminal point. In the optimal thrust pattern in both solutions, some portion of the total fuel is consumed at launch, and the rest is consumed in the proximity of the terminal point. The missile velocity is maintained to a low value before the final boost.

This thrust pattern can be approximated by a pulse motor. The optimal thrust pattern is well approximated with a booster and a sustainer at initial phase and another booster close to the terminal point without any considerable terminal velocity loss. When approximated with a more practical pulse motor composed of the two pulses of the same magnitude, terminal velocity decreases but the loss is still within 10% compared with that of the optimal pattern. Considering the practical importance of the two-pulse control, studies were conducted that optimized the impulse ratio of two pulses and their ignition intervals. It was shown that a fairly large final velocity is attained by adjusting the ignition interval and suitably controlling the angle of attack, without changing the impulse ratio. An example result showed the maximum terminal velocity obtained by a pulse motor is 25% larger than that of a single-stage motor.

Acknowledgment

The authors are indebted to Dr. S. Uehara, Director, Third Research Center TRDI of the Japan Defense Agency, for giving useful advice and discussing the paper.

References

[1]Hardtla, J. W., Milligan, K. H., and Cramer, E. J., "Design and Implementation of a Missile Guidance Law Derived from Modern Control Theory," AIAA Paper 87-2447, Aug. 1987.

[2]Calise, A. J., and Jonnalagada, V. R. P., "Pulse Motor Control for Maximizing Average Velocity," AIAA Paper 87-2510, Aug. 1987.

[3]Menon, P. K. A., Cheng, V. H. L., Lin, C. A., and Briggs, M. M., "High-Performance Missile Synthesis with Trajectory and Propulsion System Optimization," *Journal of Spacecraft and Rockets,* Vol. 24, No. 6, 1987, pp. 552–557.

[4]Imado, F., Karoda, T., and Miwa, S., "Optimal Midcourse Guidance for Medium-Range Air-to-Air Missiles," *Journal of Guidance, Control, and Dynamics,* Vol. 13, No. 4, 1990, pp. 603–608.

[5]Katzir, S., Cliff, E., and Lutze, F., "A Comparison of Dynamic Models for Optimal Midcourse Guidance," AIAA Paper 89-3481, Aug. 1989.

[6]Bryson, A. E., Jr., and Denham, W. F., "A Steepest Ascent Method for Solving Optimum Programming Problems," *Journal of Applied Mechanics,* Vol. 29, June 1962, pp. 247–257.